Optimal Persistent Monitoring Using Second-Order Agents with Physical Constraints

Yan-Wu Wang, *Senior member, IEEE,* Yao-Wen Wei, Xiao-Kang Liu, Nan Zhou, *student member, IEEE* and Christos G. Cassandras, *Fellow, IEEE*

***Abstract*—This paper addresses a one-dimensional optimal persistent monitoring problem using second-order agents. The goal is to control the movements of agents to minimize a performance metric associated with the environment (targets) over a finite time horizon. In contrast to earlier results limited to first-order dynamics for agents, we control their accelerations rather than velocities, thus leading to a better approximation of agent behavior in practice and to smoother trajectories. Bounds on both velocities and accelerations are also taken into consideration. Despite these added complications to agent dynamics, we derive a necessary condition for optimality and show that the optimal agent trajectories can be fully characterized by two parameter vectors. A gradient-based algorithm is proposed to optimize these parameters and yield a minimal performance metric. Finally, simulation examples are included to demonstrate the effectiveness of our results.**

***Index Terms*—Optimal control, persistent monitoring, second-order agent.**

I. Introduction

RECENT developments in cooperative multi-agent systems have enabled applications in which a group of autonomous agents is used to perform tasks collectively in order to optimize a global objective. In particular, persistent monitoring arises in applications such as city patrolling [1], [2], ecological surveillance [3], [4], traffic monitoring [5], [6], smart-grid security [7], [8] and ocean sampling [9], [10]. The dynamically changing environments in these applications require the agents to perpetually move in a large mission space. The challenge in this type of problems is to design the agent trajectories under physical motion constraints in order to optimize an overall performance metric.

Relevant studies on persistent monitoring problem can be categorized into two classes, namely, one with predefined trajectories [11]–[13] and one without predefined trajectories [14]–[17]. For the monitoring problem with predefined trajectories, the main challenge is to design appropriate motion laws for agents to patrol on the given trajectories. Persistent monitoring of a changing environment is addressed in [18], where the object is to control the agents' velocities to prevent the unbounded growth of an accumulation function defined on a finite number of locations. The increase or decrease of the accumulation function depends on whether the location is covered under an agent's footprint. For the monitoring problem without predefined trajectories, the main challenge is to find an optimal target visiting schedule and conditions for agents to switch if the problem is discrete [19], [20] or to search for optimal trajectories if the problem is continuous [17], [21], [22]. The latter paradigm is more flexible without predefined agent trajectories and finds wider applications, such as maneuvering targets [23], [24], detecting random events [19], [25], and monitoring dynamically changing environments [21], [26] or fields with motion constraints [27], [28]. An optimal control framework for persistent monitoring problems is proposed in [22], where an uncertainty metric is minimized subject to first-order agent dynamics. Compared with the accumulation function in [18], the uncertainty metric in [22] is more general because the detection probability of a point may vary depending on the distance between the agent and the point.

The aforementioned literature deals with the monitoring task using *first-order* agents by controlling their velocities. However, in practice agents are subjected to maximum power constraint which leads to bounds on both accelerations and velocities. In this paper, we consider *second-order* agents with such a power constraint. We control the agent accelerations rather than the velocities leading to a better approximation of agent behavior in practice and to smoother trajectories.

Based on the above discussion, we formulate the persistent monitoring problem as a minimization problem of a performance metric represented as an integral function of average uncertainty over a fixed time horizon. Specifically, this paper uses the accelerations of agents as control inputs and takes into account the physical constraints that bound both the acceleration and velocity. Through a Hamiltonian analysis, we obtain a necessary condition for optimality. The resulting optimal controller contains four modes, e.g. i) maximal acceleration mode; ii) maximal velocity mode; iii) maximal deceleration mode; iv) dwell mode. Under such an optimal control structure, the agent trajectories can be fully characterized and parameterized by the starting points of each mode and the associated dwell times. The original optimal control problem can then be transformed to a simpler parametric one and thus the search for the optimal control

This work is supported by the National Natural Science Foundation of China under Grants 61572210, 61773172, and 51537003, the Natural Science Foundation of Hubei Province of China (2017CFA035) and the academic frontier youth team of HUST.

Y.-W. Wang, Y.-W. Wei and X.-K. Liu are with the School of Automation, Huazhong University of Science and Technology, Wuhan, 430074, China, and also with the Key Laboratory of Image Processing and Intelligent Control, Ministry of Education, Huazhong University of Science and Technology, Wuhan, 430074, China (e-mail: wangyw@hust.edu.cn; weiyw@hust.edu.cn; xkliu@hust.edu.cn).

N. Zhou is with the Division of Systems Engineering, Boston University, Boston, MA 02446 USA (e-mail: nanzhou@bu.edu).

C.G. Cassandras is with the Division of Systems Engineering and Department of Electrical and Computer Engineering, Boston University, Boston, MA 02446 USA (e-mail: cgc@bu.edu).

is reduced from a functional space to some finite number of parameters along the agent trajectories. Finally, a gradient-based algorithm is proposed to minimize the performance metric and to determine the optimal trajectories.

This paper is organized as follows. Section II formulates the optimal persistent monitoring problem using second-order multi-agent systems. Subsection III-A analyzes the optimal control structure and Subsection III-B shows how to determine the optimal trajectories through a gradient-based algorithm. Simulation results are presented in Section IV to demonstrate the effectiveness of the proposed algorithm and to show the results of the persistent monitoring task. Section V concludes the paper.

II. Problem Formulation

Consider a one-dimensional (1D) mission space $[0, L]$. N cooperating agents are assigned to move on the mission space to accomplish a persistent monitoring task over the time horizon $[0, T]$. In this paper, we control the movement of each agent through its acceleration as opposed to the velocity in the first-order case. The dynamics of agent i are described by

$$\begin{cases} \dot{s}_i(t) = v_i(t), \\ \dot{v}_i(t) = u_i(t), \end{cases} \quad i = 1, 2, \ldots, N, \tag{1}$$

where $t \in [0, T]$, $s_i(t) \in [0, L]$ is the agent position, $v_i(t)$ is the velocity and $u_i(t)$ is the acceleration control input. We assume that the velocity of each agent i is bounded by

$$|v_i(t)| \le v_i^{max}, \quad i = 1, 2, \ldots, N, \tag{2}$$

and the acceleration input is bounded by

$$\mathcal{U} : \begin{cases} |u_i(t)| \le C_i^a, \text{ if } u_i(t)v_i(t) \ge 0, \\ |u_i(t)| \le C_i^d, \text{ if } u_i(t)v_i(t) < 0, \end{cases} i = 1, 2, \ldots, N, \tag{3}$$

where v_i^{max}, C_i^a and C_i^d are the maximal velocity, the maximal acceleration and the maximal deceleration respectively. Note that in the deceleration mode, the control direction is opposite to the motion direction (i.e. $u_i(t)v_i(t) < 0$). The agent dynamics under boundary constraints (2) and (3) can be rewritten as

$$\begin{cases} \dot{s}_i(t) = v_i(t), \\ \dot{v}_i(t) = \begin{cases} 0, & \text{if } |v_i(t)| = v_i^{\max} \\ & \text{and } v_i(t^+)u_i(t^+) \ge 0, \\ u_i(t), & \text{otherwise}, \end{cases} \\ i = 1, 2, \ldots, N. \end{cases} \tag{4}$$

Considering that sensors have various physical characteristics, here we model the sensing capability of the ith agent for detecting a target located at $x \in [0, L]$ by a probability function $p(s_i(t), x)$ [29] that

$$p(s_i(t), x) = \begin{cases} 1 - \frac{(x - s_i(t))^2}{r_i^2}, & \text{if } |x - s_i(t)| < r_i \\ 0, & \text{otherwise} \end{cases},$$

where r_i is the effective sensing radius. The probability that target x is sensed by all agents simultaneously can be formulated as:

$$P(S(t), x) = 1 - \prod_{i=1}^{N} [1 - p(s_i(t), x)], \tag{5}$$

where $S(t) = [s_1(t), s_2(t), \ldots, s_N(t)]$ is the position vector of all agents.

Referring to previous research, this paper adopts the definition of uncertainty from [18], [22]. A time-varying function $R(x, t)$ is defined to denote the uncertainty of target x at time t with the following properties. If target x can't be sensed by any agent, $R(x, t)$ increases with a prespecified rate $I(x)$. Meanwhile, if x is sensed with probability $P(S(t), x)$, then $R(x, t)$ increases with rate $I(x) - D(x)P(S(t), x)$, where $D(x)$ is the maximal monitoring effect on $R(x, t)$. However, if $R(x, t) = 0$ and $I(x) - D(x)P(S(t), x) < 0$, the uncertainty remains 0. The dynamics of the uncertainty function are as follows,

$$\dot{R}(x, t) = \begin{cases} 0 & \text{if } I(x) - D(x)P(S(t), x) < 0 \\ & \text{and } R(x, t) = 0, \\ I(x) - D(x)P(S(t), x) & \text{otherwise}. \end{cases} \tag{6}$$

The purpose of this persistent monitoring task is to minimize the performance metric which is defined as the average uncertainty of all targets over the time horizon $[0, T]$. In light of [22], setting $U(t) = [u_1(t), u_2(t), \ldots, u_N(t)]$, the optimal control problem is formulated as

$$\min_{U(t) \in \mathcal{U}} J = \frac{1}{M} \int_0^T \sum_{j=1}^{M} R(x_j, t) dt, \tag{7}$$

where $U(t)$ is the acceleration vector of all agents and x_j is the position of target j (point of interest) $j = 1, 2, \ldots, M$.

Remark 1. The performance metric (7) is the average over all target uncertainties instead of the average over the time horizon in [22]. In addition, $U(t)$ in this paper consists of the accelerations of agents, which is more practical than controlling velocities directly and makes it possible to keep the trajectory smooth.

III. Main Results

In this section, we focus on solving the optimal control problem (7) by finding the optimal control policy. The main challenge lies in three aspects: 1) the velocity and acceleration are bounded, thus the dynamics of agents are hybrid, 2) $R(x, t)$ has non-smooth switching dynamics as seen in (6), 3) the performance metric (7) is not a function of $U(t)$ explicitly. The work in this section contains two parts. Subsection III-A shows the characteristics of the optimal control by using a Hamiltonian analysis. Under such optimal control policies, the agent trajectories can be parameterized by a sequence of locations of control switches and the associated dwell times when an agent switches its control from $\pm C_i^d$ to 0. Thus, the performance metric in (7) can be transformed into a parametric form as we will show later in subsection III-B. A gradient-based algorithm is designed to calculate the minimal performance metric and to determine the optimal trajectory of each agent.

A. Optimal control policy

In this subsection, the optimal policy will be determined. Let the acceleration vector be denoted by

$V(t) = [v_1(t), v_2(t), \ldots, v_N(t)]$, and the uncertainty vector by $\mathfrak{R}(t) = [R(x_1,t), R(x_2,t), \ldots, R(x_M,t)]$. The performance metric in (7) will be minimized subject to the agent dynamics (1), uncertainty dynamics (6) and control constraints (3). Introducing the associated Lagrange multipliers $\lambda_u(t) = [\lambda_{u_1}(t), \lambda_{u_2}(t), \ldots, \lambda_{u_N}(t)]$, $\lambda_v(t) = [\lambda_{v_1}(t), \lambda_{v_2}(t), \ldots, \lambda_{v_N}(t)]$ and $\lambda_R(t) = [\lambda_{R_1}(t), \lambda_{R_2}(t), \ldots, \lambda_{R_M}(t)]$ with the boundary conditions $\lambda_u(T) = 0$, $\lambda_v(T) = 0$ and $\lambda_R(T) = 0$ separately. The performance metric is also subject to the velocity constraints (2) and we introduce $\mu(t) = [\mu_1(t), \mu_2(t), \ldots, \mu_N(t)]$:

$$\begin{cases} \mu_i(t) = 0, & \text{if } v_i < v^{\max}, \\ \mu_i(t) > 0, & \text{if } v_i = v^{\max}. \end{cases}$$

Then, the minimization problem (7) can be rewritten as

$$\begin{aligned} \min_{U(t)\in\mathcal{U}} J = \frac{1}{M}\int_0^T & [\mathbf{1}_M \mathfrak{R}^T(t) + \lambda_v(t)(V^T(t) - \dot{S}^T(t)) \\ & + \lambda_u(t)(U^T(t) - \dot{V}^T(t)) \\ & + \lambda_R(t)(\dot{\mathfrak{R}}^T(t) - \dot{\mathfrak{R}}^T(t)) \\ & + \mu(t)(V(t) - V^{\max})^T]dt, \end{aligned} \tag{8}$$

where $\mathbf{1}_M = [1, 1, \ldots, 1]_M$ and $V^{\max} = [v_1^{\max}, v_2^{\max}, \ldots, v_N^{\max}]$. The Hamiltonian is defined as

$$\begin{aligned} H(\mathfrak{R}, S, V, U, \lambda, t) = & \mathbf{1}_M \mathfrak{R}^T(t) + \lambda_v(t) V^T(t) \\ & + \lambda_u(t) U^T(t) + \lambda_R(t)\dot{\mathfrak{R}}^T(t) \\ & + \mu(t)(V(t) - V^{\max})^T. \end{aligned} \tag{9}$$

For simplicity, we write $H \equiv H(\mathfrak{R}, S, V, U, \lambda, t)$ and (8) can be rewritten as

$$\begin{aligned} \min_{U(t)\in\mathcal{U}} J = \frac{1}{M}\int_0^T & [H - \lambda_v(t)\dot{S}^T(t) \\ & - \lambda_u(t)\dot{V}^T(t) - \lambda_R(t)\dot{\mathfrak{R}}^T(t)]dt, \end{aligned} \tag{10}$$

Furthermore, integrate the last three terms on the right side of (10) by parts, which yields $\int_0^L \lambda_v(t)\dot{S}^T(t)dt = \lambda_v(t)S^T(t)|_0^T - \int_0^L \dot{\lambda}_v(t)S^T(t)dt$ and the same result applies for $\int_0^L \lambda_u(t)\dot{V}^T(t)$ and $\int_0^L \lambda_R(t)\dot{\mathfrak{R}}^T(t)$. Hence, combining with the boundary conditions of Lagrange multipliers, (10) can be rewritten as

$$\begin{aligned} \min_{U(t)\in\mathcal{U}} J = \frac{1}{M}\int_0^T & [H + \dot{\lambda}_v(t)S^T(t) \\ & + \dot{\lambda}_u(t)V^T(t) + \dot{\lambda}_R(t)\mathfrak{R}^T(t)]dt. \end{aligned} \tag{11}$$

Based on the optimal necessary conditions of the Hamiltonian analysis, the costates should satisfy

$$\dot{\lambda}_R(t) = -\frac{\partial H}{\partial \mathfrak{R}(t)} = -\mathbf{1}_M, \tag{12}$$

$$\dot{\lambda}_v(t) = -\frac{\partial H}{\partial S(t)} = -\lambda_R(t)\frac{\partial \dot{\mathfrak{R}}(t)}{\partial S(t)}, \tag{13}$$

$$\dot{\lambda}_u(t) = -\frac{\partial H}{\partial V(t)} = -\lambda_v(t). \tag{14}$$

Then it is ready to establish the following proposition, in which the relationships between the optimal control input and the Lagrange multipliers are revealed.

***Proposition* 1.** *For any given trajectory, the optimal control policy satisfies*

$$u_i^*(t) \in \left\{\pm C_i^a, \pm C_i^d, 0\right\}, \text{ for all } t \in [0, T]. \tag{15}$$

Proof. Let $\Gamma_0(t) = \{i | \lambda_{u_i}^*(t) = 0, i = 1, 2, \ldots, N\}$, $\Gamma_1(t) = \{i | \lambda_{u_i}^*(t) > 0, i = 1, 2, \ldots, N\}$ and $\Gamma_2(t) = \{i | \lambda_{u_i}^*(t) < 0, i = 1, 2, \ldots, N\}$. The Pontryagin Minimum Principle [30] holds for the optimal control problem (11) and asserts that

$$H(\mathfrak{R}, S, V, U^*, \lambda^*, t) = \min_{U(t)} H(\mathfrak{R}, S, V, U, \lambda^*, t),$$

where U^*, λ^* denote the vector of optimal controller and Lagrange multiplier. Clearly, it is necessary for the optimal control of agent i to satisfy

$$u_i^*(t) = -\operatorname{sgn}(\lambda_{u_i}^*(t)) \max_{u_i(t)\in\mathcal{U}} |u_i(t)|,$$

For $i \in \Gamma_1(t)$, agent i moves toward the negative direction with maximal acceleration or toward the positive direction with maximal deceleration, i.e.,

$$\begin{aligned} u_i^*(t) = -{C_i}^a, && \text{if } v_i(t) < 0, \\ u_i^*(t) = -{C_i}^d, && \text{if } v_i(t) > 0. \end{aligned}$$

Similarly, for $i \in \Gamma_2(t)$ the optimal control of agent i satisfies

$$\begin{aligned} u_i^*(t) = {C_i}^a, && \text{if } v_i(t) > 0, \\ u_i^*(t) = {C_i}^d, && \text{if } v_i(t) < 0. \end{aligned}$$

It is possible(see Ch.3 in [31]) that there are some agents $i \in \Gamma_0(t)$ at some time intervals $[t_1, t_2]$. For these $i \in \Gamma_0(t)$, $\lambda_{u_i}^*(t)u_i(t) = 0$ which is omitted in the above analysis. From (9), $H(\mathfrak{R}, S, V, U, \lambda, t)$ is not an explicit function of t and $H(\mathfrak{R}, S, V, U^*, \lambda^*, t) \equiv C$ is constant [32]. Therefore, $\frac{dH}{dt} = 0$ which gives

$$\begin{aligned} \frac{dH}{dt} = & \mathbf{1}_M \dot{\mathfrak{R}}^T(t) + (\dot{\lambda}_v(t)V^T(t) + \lambda_v(t)\dot{V}^T(t)) \\ & + (\dot{\lambda}_u(t)U^T(t) + \lambda_u(t)\dot{U}^T(t)) \\ & + (\dot{\lambda}_R(t)\dot{\mathfrak{R}}^T(t) + \lambda_R(t)\ddot{\mathfrak{R}}^T(t)) \\ & + \dot{\mu}(t)(V(t) - V^{max})^T + \mu(t)U^T(t). \end{aligned} \tag{16}$$

Meanwhile, based on the necessary conditions (12) and (14),

$$\mathbf{1}_M \dot{\mathfrak{R}}^T(t) + \dot{\lambda}_R(t)\dot{\mathfrak{R}}^T(t) = 0,$$

$$\lambda_v(t)\dot{V}^T(t) + \dot{\lambda}_u(t)U^T(t) = 0,$$

which gives

$$\begin{aligned} \frac{dH}{dt} = & \dot{\lambda}_v(t)V^T(t) + \lambda_R(t)\ddot{\mathfrak{R}}^T(t) + \lambda_u(t)\dot{U}^T(t) \\ & + \dot{\mu}(t)(V(t) - V^{max})^T + \mu(t)U^T(t). \end{aligned} \tag{17}$$

For those agents $i \in \Gamma_0(t)$, we have $\lambda_{u_i}(t) = 0$, so that $\sum_{i\in\Gamma_0(t)} \lambda_{u_i}(t)\dot{u}_i(t) = 0$, and for those agents $i \in \Gamma_1(t) \cup \Gamma_2(t)$, we have $u_i(t) = \pm C_i^a$ or $\pm C_i^d, \dot{u}_i(t) = 0$ and $\sum_{i\in\Gamma_1(t)\cup\Gamma_2(t)} \lambda_{u_i}(t)\dot{u}_i(t) = 0$. The above analysis suggests that $\lambda_u(t)\dot{U}^T(t) = 0$. According to (14), if $i \in \Gamma_0(t), \lambda_{u_i}(t) =$

0, $\dot{\lambda}_{u_i}(t) = 0 = -\lambda_{v_i}(t)$. Thus, for any time instant, (17) is reduced to

$$\frac{dH}{dt} = \sum_{i\in\Gamma_1(t)\cup\Gamma_2(t)} \dot{\lambda}_{v_i}(t)v_i(t) + \lambda_R(t)\ddot{\mathfrak{R}}^T(t) + \dot{\mu}(t)(V(t) - V^{max})^T + \mu(t)U^T(t). \qquad (18)$$

From (6), since $\dot{R}(s(t), x)$ is not an explicit function of t, we have

$$\ddot{\mathfrak{R}}(t) = \frac{d(\dot{\mathfrak{R}}(t))}{d(S(t))}\dot{S}^T(t).$$

From (13), it follows that for $i \in \Gamma_1(t) \cup \Gamma_2(t)$,

$$\dot{\lambda}_{v_i}(t)v_i(t) + \lambda_{R_i}(t)\frac{d(\dot{\mathfrak{R}}(t))}{d(s_i(t))}\dot{s}_i(t) = 0.$$

which provides the fact that

$$\frac{dH}{dt} = \sum_{i\in\Gamma_0(t)} \lambda_{R_i}(t)\frac{d(\dot{\mathfrak{R}}(t))}{d(s_i(t))}\dot{s}_i(t) + \dot{\mu}(t)(V(t) - V^{max})^T + \mu(t)U^T(t). \qquad (19)$$

If the state evolves in an interior arc of velocity constraint (2), i.e., $v_i(t) < v_i^{max}$ and $\mu(t) = 0, \dot{\mu}(t) = 0$. Otherwise, the state evolves in the boundary arc of (2), i.e., $|v_i(t)| \equiv v_i^{max}$, then $u_i(t) = 0$. Then, it can be obtained that $\dot{\mu}(t)(V(t) - V^{max})^T + \mu(t)U^T(t) = 0$. From (19),

$$\frac{dH}{dt} = \sum_{i\in\Gamma_0(t)} \lambda_{R_i}(t)\frac{d(\dot{\mathfrak{R}}(t))}{d(s_i(t))}\dot{s}_i(t). \qquad (20)$$

Thus, to ensure (20) holds at all $t \in [0, T]$, $\dot{s}_i(t) = 0$ for those $i \in \Gamma_0(t)$ which means $v_i(t) = 0, u_i(t) = 0$.

Note also from (4), $u_i(t) = 0$ if $|v_i(t)| = v_i^{max}$ for a time period. Based on the above analysis, (15) holds, which completes the proof. ■

From *Proposition 1*, $u_i^*(t) \in \{\pm C_i^a, \pm C_i^d, 0\}$, the optimal control requires the agents to move with maximal acceleration or fixed maximal velocity or maximal deceleration or remain at rest. To be more specific, the motion of an agent, moving from one point to another, may include four modes: i) maximal acceleration mode: the agent moves with maximal acceleration from one point to another, where the control direction is agree with the motion direction; ii) maximal velocity mode: the agent moves at a fixed maximal velocity for a period of time larger than zero; iii) maximal deceleration mode: the agent moves with maximal deceleration, where the control direction is opposite to the motion direction; iv) dwell mode: the agent dwells at some points for some time (possibly zero). The resulting optimal agent trajectories can be fully characterized by the starting points and end points of each mode and the dwell times associated with each dwell mode.

Remark 2. Proposition 1 reveals the agent's optimal acceleration for any given trajectory. From the optimal analysis of Proposition 1, when the maximal velocity constraints is not active the associate Lagrange multiplier can only be $\lambda_{u_i}(t) > 0, < 0, = 0$, the agent's optimal acceleration should be maximal acceleration or deceleration, or zero acceleration (with zero velocity), which leads to the maximal acceleration or deceleration mode, or dwell mode respectively. When the maximal velocity constraints is active, i.e. $v_i^*(t) = v_i^{max}, u_i^*(t) = 0$ for some time intervals, which leads to the maximal velocity mode.

In the following, we will show that the agents will never arrive at the boundary point 0 or L.

Proposition 2. *On an optimal trajectory the agents will never visit* 0 *and* L*, i.e.,* $\forall\, t \in (0, T), i \in \{1, 2, \ldots, N\}$*,* $s_i^*(t) \neq 0$ *and* $s_i^*(t) \neq L$*.*

Proof. Suppose at $t = t_0 < T$, $s_i(t_0) = 0$ and $s_i(t_0^-) > 0$, then $v_i(t_0^-) < 0$ and $u_i(t_0^-) = C_i^d > 0$. Following the standard optimal control analysis [31], if $-s_i(t_0) \leq 0$ holds, $\lambda_{v_i}(t)$ may experience a discontinuity so that

$$\lambda_{v_i}(t_0^-) = \lambda_{v_i}(t_0^+) - \pi_i \qquad (21)$$

where $\pi_i \geq 0$ is a scalar constant and there surely exist some $\pi_i > 0$. From (13), it is obvious that $\lambda_{v_i}(t)$ is a continuous function, which is conflict with (21) above. The same argument can be made for $s_i(t_0) = L$. The proof is thus completed. ■

For agent i, define the dwelling points $\theta_i = [\theta_{i1}, \theta_{i2}, \ldots, \theta_{iK_i}]$ in $[0, L]$ at which $v_i(t) = 0, u_i(t) = 0$ and $\omega_i = [\omega_{i1}, \omega_{i2}, \ldots, \omega_{iK_i}]$ to be the associated dwelling times at such K_i dwelling points. Further define the switching points $\theta_{ik_i}^a$ (ending points of maximal acceleration mode), and $\theta_{ik_i}^d$ (starting points of maximal deceleration mode) between θ_{ik_i} and $\theta_{i(k_i+1)}$, $k_i = 1, 2, \ldots, K_i - 1$. For $\theta_{ik_i}^a = \theta_{ik_i}^d$ being a same point, at this point $u_i(t)$ changes from $u_i(t) = \pm C_i^a$ to $u_i(t) \mp C_i^d$ directly. For $\theta_{ik_i}^a \neq \theta_{ik_i}^d$, agent i moves at fixed maximal velocity between $\theta_{ik_i}^a$ and $\theta_{ik_i}^d$, $u_i(t)$ changes from $u_i(t) = \pm C_i^a$ to $u_i(t) = 0$ at $\theta_{ik_i}^a$ and from $u_i(t) = 0$ to $u_i(t) \mp C_i^d$ at $\theta_{ik_i}^d$.

Remark 3. Note that once the dwelling points θ_i are determined, the acceleration, deceleration and the possibly maximum velocity modes between these points can be subsequently calculated. Therefore, if the dwelling points and the dwelling times are determined, the trajectory of agent i will be fully determined and represented as $[\theta_i, \omega_i]$, and the trajectories of all agents can be represented as $[\theta, \omega]$ where $\theta = [\theta_1, \theta_2, \ldots, \theta_N], \omega = [\omega_1, \omega_2, \ldots, \omega_N]$.

To proceed, the existence of the maximum velocity modes will be analyzed in the following proposition.

Proposition 3. *The maximum velocity mode exists between* θ_{ih} *and* $\theta_{i(h+1)}$ *when agent i moves from* θ_{ih} *to* $\theta_{i(h+1)}$ *if and only if*

$$|\theta_{i(h+1)} - \theta_{ih}| > \frac{{v_i^{\max}}^2}{2C_i^a} + \frac{{v_i^{\max}}^2}{2C_i^d}. \qquad (22)$$

Proof. Note that θ_{ih} and $\theta_{i(h+1)}$ are both dwelling points at which $v_i(t) = 0$. The time it takes for the velocity of agent i to increase from 0 to $v_i^{\max}$ with the maximal acceleration C_i^a is $\frac{v_i^{\max}}{C_i^a}$ and the time it takes for the velocity of agent i to decrease from $v_i^{\max}$ to 0 with the maximal deceleration C_i^d is $\frac{v_i^{\max}}{C_i^d}$. The average velocity of both the uniform acceleration and deceleration process is $\frac{v_i^{\max}}{2}$. Therefore, the shortest distance between θ_{ih} and $\theta_{i(h+1)}$ for agent i to reach the maximal velocity is

$$\frac{v_i^{\max}}{C_i^a}\frac{v_i^{\max}}{2}+\frac{v_i^{\max}}{C_i^d}\frac{v_i^{\max}}{2}.$$

Hence, the maximal velocity mode exists between θ_{ih} and $\theta_{i(h+1)}$ if and only if (22) holds. ■

The next subsection is devoted to determining the optimal dwelling points and the corresponding optimal dwelling times, so as to determine the optimal trajectory.

B. Optimal trajectory

Since the agent trajectories are represented as $[\theta,\omega]$, combining with *Proposition 1*, the controller $U(t)$ is also determined by $[\theta,\omega]$. In other words, the problem is simplified as a parametric minimization problem of finding the optimal dwelling points and the optimal dwelling times. Thus, the objective is to determine $[\theta,\omega]$ satisfying

$$\min_{U(t)\in\mathcal{U}} J=\min_{[\theta,\omega]} J(\theta,\omega).$$

A gradient-based iterative algorithm is designed as follows,

$$\begin{aligned}[\theta(m),\omega(m)]=&[\theta(m-1),\omega(m-1)] \\ &+[\tilde{\theta},\tilde{\omega}]\nabla J(\theta(m-1),\omega(m-1)),\end{aligned} \tag{23}$$

where $m=1,2,\dots$ is the index of iterations, $[\tilde{\theta},\tilde{\omega}]$ is the step-size of the iterative algorithm and $\nabla J(\theta(m),\omega(m))=[\frac{\partial J(\theta(m),\omega(m))}{\partial\theta(m)},\frac{\partial J(\theta(m),\omega(m))}{\partial\omega(m)}]^T$ is the gradient of J with respect to $\theta(m)$ and $\omega(m)$. The trajectory parameters are optimized through (23) by iterations with the terminal condition:

$$|J(\theta(m+1),\omega(m+1))-J(\theta(m),\omega(m))|<\varepsilon, \tag{24}$$

where $\varepsilon>0$ is a predetermined constant.

Therefore, what is left is to calculate $\nabla J(\theta,\omega)$. According to (6), the uncertainty dynamics define a switching function. Define a time sequence to describe the switching instants of $\dot{\mathfrak{R}}(t)$, $\tau(\theta,\omega)=\{\tau_l(\theta,\omega)\}, l=0,1,\dots,\mathcal{L}-1$, with boundary conditions $\tau_0(\theta,\omega)=0,\tau_{\mathcal{L}}(\theta,\omega)=T$. Thus, the performance metric (7) can be represented as

$$J(\theta,\omega)=\frac{1}{M}\sum_{l=0}^{\mathcal{L}-1}\int_{\tau_l(\theta,\omega)}^{\tau_{l+1}(\theta,\omega)}\sum_{j=1}^{M}R(x_j,t)dt.$$

Then, $\nabla J(\theta,\omega)$ can be rewritten as

$$\nabla J(\theta,\omega)=\frac{1}{M}\sum_{l=0}^{\mathcal{L}-1}\sum_{j=1}^{M}\int_{\tau_l(\theta,\omega)}^{\tau_{l+1}(\theta,\omega)}\nabla R(x_j,t)dt, \tag{25}$$

where $\nabla R(x_j,t)=[\frac{\partial R(x_j,t)}{\partial\theta},\frac{\partial R(x_j,t)}{\partial\omega}]$. Therefore, in order to compute $\nabla J(\theta,\omega)$ we need to first compute $\nabla R(x_j,t)$.

It's obvious that $R(x_j,t)$ is not an explicit function of (θ,ω). Therefore, transforming the performance metric in (7) to a function of (θ,ω) is necessary in the following analysis. Note that from the motion law in *Proposition 1*, the optimal trajectories are described by $[\theta,\omega]$, therefore, the positions of agents are also represented by $[\theta,\omega]$, i.e., the position vector is $S(t)\equiv S(t,(\theta,\omega))$. The following discussion is carried out in three steps, in which a numerical computation method is utilized to calculate $\nabla R(x_j,t)$. Let $t_k=k\delta, k=1,2\dots$ be the computation time sequence in $[0,T]$, where the computation step δ is sufficiently small and $t_0=0$.

Step 1). For two adjacent instants t_k and t_{k-1}, there are two cases to be discussed.

Case 1.1 No switches between t_k and t_{k-1}. In this case, $t_{k-1},t_k\in(\tau_l(\theta,\omega),\tau_{l+1}(\theta,\omega))$ and the dynamics of target uncertainties do not switch. According to (6), utilizing the Euler method $\nabla R(x_j,t_k)=\nabla R(x_j,t_{k-1})+\nabla\dot{R}(x_j,t_{k-1})\delta$,

$$\begin{aligned}&\nabla R(x_j,t_k)=\nabla R(x_j,t_{k-1}) \\ &-\begin{cases}0, & \text{if } \dot{R}(x_j,t_{k-1})=0,\\ D(x_j)\frac{\partial P(S(t_{k-1}),x_j)}{\partial S(t_{k-1})}\nabla S(t_{k-1})\delta, & \text{otherwise},\end{cases}\end{aligned} \tag{26}$$

where $\nabla S(t_{k-1})=(\frac{\partial S(t_{k-1})}{\partial\theta},\frac{\partial S(t_{k-1})}{\partial\omega})$ needs further to be calculated in Step 2) and 3).

Case 1.2 There exists a switch between t_k and t_{k-1}. In this case, t_{k-1},t_k satisfy $t_{k-1}\le\tau_l(\theta,\omega)\le t_k$. Suppose it is target j^* that switches its dynamics: $\dot{R}(x_{j^*},t)$ switches from 0 to $I(x_{j^*})-D(x_{j^*})P(S(t),x_{j^*})$, or from $I(x_{j^*})-D(x_{j^*})P(S(t),x_{j^*})$ to 0 at $\tau_l(\theta,\omega)$. Therefore, there are two subcases to be discussed.

Before the analysis, we introduce the Infinitesimal Perturbation Analysis method [22], [33] to specify how the arguments θ influences the system state $s(\theta,t)$, ultimately, how they influence the performance metric which can be expressed in terms of such arguments. Let $\{\tau_l(\theta)\}, l=0,1,\dots,\mathcal{L}-1$, denote the occurrence time of all events in the state trajectory. For convenience, we set $\tau_0=0$ and $\tau_{\mathcal{L}}=T$. For $t\in[\tau_{l-1},\tau_l)$, based on the Jacobian matrix notation, we define $s'(t)\equiv\frac{\partial s(\theta,t)}{\partial\theta}$ and $\dot{s}(t)=f_l(s,\theta,t)$. In the following we use $f_l(t)$ for simplicity. Since t is independent on θ,

$$\frac{d}{dt}s'(t)=\frac{\partial f_l(t)}{\partial s}s'(t)+\frac{\partial f_l(t)}{\partial\theta}, \tag{27}$$

with boundary condition:

$$s'(\tau_l^+)=s'(\tau_l^-)+[f_{l-1}(\tau_l^-)-f_l(\tau_l^+)]\frac{\partial\tau_l(\theta)}{\partial\theta}. \tag{28}$$

Then, let's focus on the gradient $\frac{\partial\tau_l(\theta)}{\partial\theta}$. If there exists a continuously differentiable function $g_l(s(\theta,t),\theta)$, such that $g_l(s(\theta,\tau_l),\theta)=0$ for any τ_l (in the following we use g_l for simplicity) holds, then we have

$$\begin{aligned}\frac{d}{d\theta}g_l&=\frac{\partial g_l}{\partial s}[\frac{\partial s}{\partial\theta}+\frac{\partial s}{\partial\tau_l}\frac{\partial\tau_l}{\partial\theta}]+\frac{\partial g_l}{\partial\theta}\\ &=\frac{\partial g_l}{\partial s}[s'(\tau_l)+f_l(\tau_l)\frac{\partial\tau_l}{\partial\theta}]+\frac{\partial g_l}{\partial\theta}\\ &=0,\end{aligned}$$

Thus, if $\frac{\partial g_l}{\partial s}f_l(\tau_l^-)\neq0$,

$$\frac{\partial\tau_l(\theta)}{\partial\theta}=-[\frac{\partial g_l}{\partial s}f_l(\tau_l^-)]^{-1}(\frac{\partial g_l}{\partial\theta}+\frac{\partial g_l}{\partial s}s'(\tau_l^-)). \tag{29}$$

We are now ready to discuss the two subcases.

Case 1.2.1 $\dot{R}(x_{j^*},t_{k-1})<0$ switches to $\dot{R}(x_{j^*},t_k)=0$. In this case, $R(x_{j^*},t)$ satisfies the *endogenous* condition in [22], (29) applies with $g_l=R(x_{j^*},\tau_l)=0$, we get

$$\nabla t_k=-\frac{\nabla R(x_{j^*},t_{k-1})}{I(x_{j^*})-D(x_{j^*})P(S(t_{k-1}),x_{j^*})},$$

and combine with (28) that

$$\nabla R(x_{j^*}, t_k) = 0. \tag{30}$$

Case 1.2.2 $\dot{R}(x_{j^*}, t_{k-1}) = 0$ switches to $\dot{R}(x_{j^*}, t_k) > 0$. In this case, $\dot{R}(x_{j^*}, t)$ is continuous, so that $f_l(\tau_l^+) = f_l(\tau_l^-)$ in (28) applied to $R(x_{j^*}, t)$ we have

$$\nabla R(x_{j^*}, t_k) = \nabla R(x_{j^*}, t_{k-1}). \tag{31}$$

Note that it is impossible for the uncertainty dynamics to switch from $\dot{R}(x_{j^*}, t_{k-1}) > 0$ to $\dot{R}(x_{j^*}, t_k) = 0$; this is because if $\dot{R}(x_{j^*}, t_{k-1}) > 0$, $\dot{R}(x_{j^*}, t_k) > \dot{R}(x_{j^*}, t_{k-1}) > 0$, the uncertainty dynamics remain $\dot{R}(x_{j^*}, t_k) > 0$ and switching does not take place. Also, it is impossible for the dynamics to switch from $\dot{R}(x_{j^*}, t_{k-1}) = 0$ to $\dot{R}(x_{j^*}, t_k) < 0$.

Step 2). In this step, case 1.1 will be further discussed.

Based on (26), the remaining work is to calculate $\nabla S(t_k)$. From the agent dynamics (4), $S(t)$ is a continuously differentiable function. According to the optimal control structure in Proposition 1, the dynamics of $S(t)$ fall into four cases. Between each adjacent dwelling points $[\theta_{ih}, \theta_{ih+1}]$, we define t_{ih} as the time instant when agent i leaves from θ_{ih} and $t_{ih}^a, t_{ih}^u, t_{ih}^d$ are the time intervals that agent i spends in the hth acceleration mode, maximal velocity mode and deceleration mode, respectively. Then, we have

$$t_{ih} = \sum_{q=1}^{h-1} [\omega_{iq} + t_{iq}^a + t_{iq}^u + t_{iq}^d] + \omega_{ih}. \tag{32}$$

To proceed, the mode of agent i will firstly be discussed from the hth dwelling point θ_{ih} to the $(h+1)$th dwelling point $\theta_{i(h+1)}$, which is illustrated in Fig. 1 (in the figure, the case of $\theta_{ih} < \theta_{i(h+1)}$ is illustrated; the opposite case is similar).

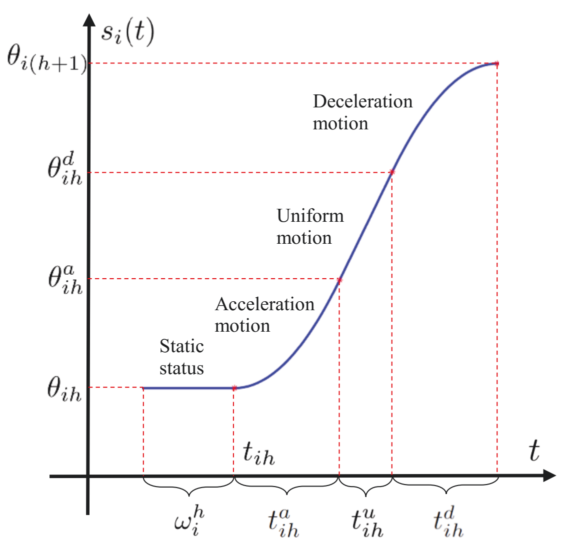

Fig. 1. The schematic for the motion of agent i.

According to the kinematic laws of uniformly variable motion and uniform motion, the motion of agent i between θ_{ih} and $\theta_{i(h+1)}$ is obtained as follows.

Case 2.1 For the hth maximal acceleration mode, $s_i(t) \in [\theta_{ih}, \theta_{ih}^a), t \in [t_{ih}, t_{ih} + t_{ih}^a)$, then,

$$s_i(t) = \theta_{ih} + \text{sgn}(\theta_{i(h+1)} - \theta_{ih})\frac{1}{2}C_i^a(t - t_{ih})^2, \tag{33}$$

$$\nabla s_i(t) = \nabla\theta_{ih} - \text{sgn}(\theta_{i(h+1)} - \theta_{ih})v_i(t)\nabla t_{ih}. \tag{34}$$

Case 2.2 For the hth maximal velocity mode, the existence depends on the length of $|\theta_{ih+1} - \theta_{ih}|$ as presented in Proposition 3. If the hth maximal velocity mode exists, the two points θ_{ih}^a and θ_{ih}^d are not the same and $t_{ih}^u > 0$. Thus, for $s_i(t) \in [\theta_{ih}^a, \theta_{ih}^d), t \in [t_{ih} + t_{ih}^a, t_{ih} + t_{ih}^a + t_{ih}^u)$,

$$s_i(t) = \theta_{ih}^a + \text{sgn}(\theta_{i(h+1)} - \theta_{ih})v_i^{\max}(t - t_{ih} - t_{ih}^a), \tag{35}$$

$$\nabla s_i(t) = \nabla\theta_{ih}^a - \text{sgn}(\theta_{i(h+1)} - \theta_{ih})v_i^{\max}\nabla(t_{ih} + t_{ih}^a). \tag{36}$$

Case 2.3 For the hth maximal deceleration mode, $s_i(t) \in [\theta_{ih}^d, \theta_{i(h+1)}), t \in [t_{ih} + t_{ih}^a + t_{ih}^u, t_{i(h+1)} - \omega_{i(h+1)})$, then,

$$\begin{aligned} s_i(t) = \theta_{ih}^d &+ \text{sgn}(\theta_{i(h+1)} - \theta_{ih})[v_i^{\max}(t - t_{ih} - t_{ih}^a - t_{ih}^u) \\ &- \frac{1}{2}C_i^d(t - t_{ih} - t_{ih}^a - t_{ih}^u)^2], \end{aligned} \tag{37}$$

$$\begin{aligned} \nabla s_i(t) = \nabla\theta_{ih}^d &- \text{sgn}(\theta_{i(h+1)} - \theta_{ih})v_i(t) \\ &\times \nabla(t_{ih} + t_{ih}^a + t_{ih}^u). \end{aligned} \tag{38}$$

Case 2.4 For the hth dwell mode, $s_i(t) = \theta_{ih}, t \in [t_{ih} - \omega_{ih}, t_{ih})$, then,

$$\nabla s_i(t) = \nabla\theta_{ih}. \tag{39}$$

Step 3). In (34),(36),(38) and (39), ∇t_{ih}^a, ∇t_{ih}^u, $\nabla\theta_{ih}$, $\nabla\theta_{ih}^a$, $\nabla\theta_{ih}^d$ and ∇t_{ih} remain to be calculated. From (32),

$$\nabla t_{ih} = \sum_{q=1}^{h-1} \nabla[\omega_{iq} + t_{iq}^a + t_{iq}^u + t_{iq}^d] + \nabla\omega_{ih}, \tag{40}$$

and obviously,

$$\frac{\partial\omega_h}{\partial\theta_{iq}} = 0, \tag{41}$$

and

$$\begin{cases} \frac{\partial\omega_{ih}}{\partial\omega_{ih}} = 1, \\ \frac{\partial\omega_{ih}}{\partial\omega_q} = 0, q = 1, \ldots, h-1, h+1, \ldots, K_i. \end{cases} \tag{42}$$

From Proposition 3, the existence of the maximum velocity modes is determined by the length of $|\theta_{i(h+1)} - \theta_{ih}|$. Thus, the motion between θ_{ih} and $\theta_{i(h+1)}$ can be divided into two categories according to Proposition 3.

Case 3.1 If $t_{ih}^u > 0$, the maximal velocity mode exists at a time interval $[t_{ih} + t_{ih}^a, t_{ih} + t_{ih}^a + t_{ih}^u)$(refer to Fig. 1) when agent i moves from θ_{ih} to $\theta_{i(h+1)}$.

In this case, agent i firstly moves from θ_{ih} to θ_{ih}^a with fixed acceleration C_i^a, then moves to θ_{ih}^d with fixed velocity v_i^{max}, at last moves to $\theta_{i(h+1)}$ with fixed deceleration C_i^d. According to the kinematics law, the following conditions hold:

$$\begin{cases} t_{ih}^a = \frac{v_i^{\max}}{C_i^a}, \\ t_{ih}^d = \frac{v_i^{\max}}{C_i^d}, \\ t_{ih}^u = \frac{|\theta_{i(h+1)} - \theta_{ih}| - (t_{ih}^a\frac{v_i^{\max}}{2} + t_{ih}^d\frac{v_i^{\max}}{2})}{v_i^{\max}}. \end{cases} \tag{43}$$

Therefore, taking the derivative with respect to the parameters, we obtain:

$$\begin{cases} \nabla t_{ih}^a = 0, \\ \nabla t_{ih}^d = 0, \end{cases} \tag{44}$$

$$\begin{cases} \frac{\partial t_{ih}^u}{\partial \theta_{i(h+1)}} = \frac{\mathrm{sgn}(\theta_{i(h+1)}-\theta_{ih})}{v_i^{\max}}, \\ \frac{\partial t_{ih}^u}{\partial \theta_{ih}} = -\frac{\mathrm{sgn}(\theta_{i(h+1)}-\theta_{ih})}{v_i^{\max}}, \\ \frac{\partial t_{ih}^u}{\partial \theta_{iq}} = 0, q = 1, \dots, h-1, h+2, K_i, \end{cases} \tag{45}$$

and

$$\frac{\partial t_{ih}^u}{\partial \omega_{iq}} = 0, q = 1, \dots, K_i. \tag{46}$$

In addition, the associated control switching point from maximal acceleration mode to maximal velocity mode is θ_{ih}^a and from maximal velocity mode to maximal deceleration mode is θ_{ih}^d which can be calculated as follows. The switching points between θ_{ih} and $\theta_{i(h+1)}$ are $\theta_{ih}^a, \theta_{ih}^d$,

$$\theta_{ih}^a = \theta_{ih} + \mathrm{sgn}(\theta_{i(h+1)} - \theta_{ih}) t_{ih}^a \frac{v_i^{\max}}{2},$$

$$\theta_{ih}^d = \theta_{i(h+1)} - \mathrm{sgn}(\theta_{i(h+1)} - \theta_{ih}) t_{ih}^d \frac{v_i^{\max}}{2}. \tag{47}$$

Subsequently,

$$\begin{cases} \frac{\partial \theta_{ih}^a}{\partial \theta_{ih}} = 1, \\ \frac{\partial \theta_{ih}^a}{\partial \theta_{iq}} = 0, q = 1, \dots, h-1, h+1, \dots, K_i, \end{cases} \tag{48}$$

$$\frac{\partial \theta_{ih}^a}{\partial \omega_{iq}} = 0, q = 1, \dots, K_i, \tag{49}$$

$$\begin{cases} \frac{\partial \theta_{ih}^d}{\partial \theta_{i(h+1)}} = 1, \\ \frac{\partial \theta_{ih}^d}{\partial \theta_{iq}} = 0, q = 1, \dots, h, h+2, \dots, K_i, \end{cases} \tag{50}$$

and

$$\frac{\partial \theta_{ih}^d}{\partial \omega_{iq}} = 0, q = 1, \dots, K_i. \tag{51}$$

Case 3.2 If $t_{ih}^u = 0$, the maximal velocity mode does not exist when agent i moves from θ_{ih} to $\theta_{i(h+1)}$. The velocity of agent i does not have enough time to accelerate to v_i^{max} or it can increase to v_i^{max} but then decreases immediately.

In this case, agent i leaves from θ_{ih} with acceleration C_i^a until θ_{ih}^a ($\theta_{ih}^a = \theta_{ih}^d$) and then moves with deceleration C_i^d until $\theta_{i(h+1)}$. According to the kinematics law of uniformly variable motion, the following conditions hold:

$$\begin{cases} C_i^a t_{ih}^a = C_i^d t_{ih}^d, \\ \frac{1}{2} C_i^a (t_{ih}^a)^2 + \frac{1}{2} C_i^d (t_{ih}^d)^2 = |\theta_{i(h+1)} - \theta_{ih}|. \end{cases} \tag{52}$$

Solving (52) in terms of control switching time t_{ih}^a and t_{ih}^d, we have

$$\begin{cases} t_{ih}^a = \sqrt{\frac{2C_i^d}{C_i^a (C_i^a + C_i^d)} |\theta_{i(h+1)} - \theta_{ih}|}, \\ t_{ih}^d = \sqrt{\frac{2C_i^a}{C_i^d (C_i^d + C_i^a)} |\theta_{i(h+1)} - \theta_{ih}|}. \\ t_{ih}^u = 0. \end{cases} \tag{53}$$

Taking the derivative we obtain

$$\nabla t_{ih}^u = 0. \tag{54}$$

$$\begin{cases} \frac{\partial t_{ih}^a}{\partial \theta_{i(h+1)}} = \sqrt{\frac{2C_i^d}{C_i^a (C_i^a + C_i^d)}} \frac{\mathrm{sgn}(\theta_{i(h+1)}-\theta_{ih})}{2\sqrt{|\theta_{i(h+1)}-\theta_{ih}|}}, \\ \frac{\partial t_{ih}^a}{\partial \theta_{ih}} = -\sqrt{\frac{2C_i^d}{C_i^a (C_i^a + C_i^d)}} \frac{\mathrm{sgn}(\theta_{i(h+1)}-\theta_{ih})}{2\sqrt{|\theta_{i(h+1)}-\theta_{ih}|}}, \\ \frac{\partial t_{ih}^a}{\partial \theta_{iq}} = 0, q = 1, \dots, h-1, h+2, \dots, K_i, \end{cases} \tag{55}$$

$$\frac{\partial t_{ih}^a}{\partial \omega_{iq}} = 0, q = 1, \dots, K_i, \tag{56}$$

$$\begin{cases} \frac{\partial t_{ih}^d}{\partial \theta_{i(h+1)}} = \sqrt{\frac{2C_i^d}{C_i^a (C_i^a + C_i^d)}} \frac{\mathrm{sgn}(\theta_{i(h+1)}-\theta_{ih})}{2\sqrt{|\theta_{i(h+1)}-\theta_{ih}|}}, \\ \frac{\partial t_{ih}^d}{\partial \theta_{ih}} = -\sqrt{\frac{2C_i^d}{C_i^a (C_i^a + C_i^d)}} \frac{\mathrm{sgn}(\theta_{i(h+1)}-\theta_{ih})}{2\sqrt{|\theta_{i(h+1)}-\theta_{ih}|}}, \\ \frac{\partial t_{ih}^d}{\partial \theta_{iq}} = 0, q = 1, \dots, h-1, h+2, \dots, K_i, \end{cases} \tag{57}$$

and

$$\frac{\partial t_{ih}^d}{\partial \omega_{iq}} = 0, q = 1, \dots, K_i. \tag{58}$$

Moreover, in this case, $\theta_{ih}^a = \theta_{ih}^d$,

$$\theta_{ih}^a = \theta_{ih} + \mathrm{sgn}(\theta_{i(h+1)} - \theta_{ih}) \frac{1}{2} C_i^a {t_{ih}^a}^2, \tag{59}$$

$$\nabla \theta_{ih}^a = \nabla \theta_{ih} + \mathrm{sgn}(\theta_{i(h+1)} - \theta_{ih}) C_i^a t_{ih}^a \nabla t_{ih}^a.$$

Replacing ∇t_{ih}^a with (55) and (56),

$$\begin{cases} \frac{\partial \theta_{ih}^a}{\partial \theta_{ih}} = 1 - \frac{C_i^d}{(C_i^a + C_i^d)}, \\ \frac{\partial \theta_{ih}^a}{\partial \theta_{i(h+1)}} = \frac{C_i^d}{(C_i^a + C_i^d)}, \\ \frac{\partial \theta_{ih}^a}{\partial \theta_{iq}} = 0, q = 1, \dots, h-1, h+1, \dots, K_i. \end{cases} \tag{60}$$

$$\frac{\partial \theta_{ih}^a}{\partial \omega_{iq}} = 0, q = 1, \dots, K_i. \tag{61}$$

This ends the analysis of Step 3) in which $\nabla t_{ih}^a, \nabla t_{ih}^u, \nabla \theta_{ih}, \nabla \theta_{ih}^a, \nabla \theta_{ih}^d$ and ∇t_{ih} are obtained. In addition, for $k \neq i$ and $\frac{\partial s_i(t)}{\partial \theta_k} = 0, \frac{\partial s_i(t)}{\partial \omega_k} = 0$.

Remark 4. For a certain trajectory of agent i, the total number of dwelling points K_i is determined by the time horizon T. Based on the analysis of Step 3), the dwelling points its dwelling time will be updated constantly until the optimal trajectory is obtained. Therefore, the total number of dwelling points K_i will change with the iterative process of trajectory.

In summary, Steps 2) and 3) show the calculation of $\nabla S(t)$.

Based on the above analysis, $\nabla J(\theta, \omega)$ is obtained and the gradient-based iterative algorithm is designed as illustrated in Algorithm 1.

C. Collision avoidance

Note that in [22], the optimal trajectory will avoid the collision as shown in Proposition III.4 of [22]. However, in this paper, the agent will ensure a deceleration process before it can fully stop and change its moving direction, which will bring cost, therefore, theoretically it may be a better strategy for the agent to collide its neighbor with a certain velocity rather than it stops before the collision. Consequently, we need to take a certain strategy in the algorithm to avoid the collision. To do so, we present Algorithm 3.

Algorithm 1 Gradient-based iteration algorithm

Initialization: The maximal velocities, accelerations and decelerations of agents, v_i^{max}, C_i^a, C_i^d. The initial trajectories of all agents $[\theta(0), \omega(0)]$, a given terminal condition ε, a sufficient small computation step δ, and the index of iterations $m = 1$.

repeat
  Calculate $S(t)$ using (4)(15) and $[\theta(m), \omega(m)]$;
  for $j = 1 : M$ **do**
    Calculate $\dot{R}(x_j, t)$ according to (6);
    if $\dot{R}(x_j, t)$ switches **then**
      Calculate $\nabla R(x_j, t)$ according to (30) and (31);
    else
      if $\dot{R}(x_j, t)$ does not switch **then**
        Calculate $\nabla R(x_j, t)$ according to (26) by activating Algorithm 2 to calculate $\nabla S(t)$;
      end if
    end if
  end for
  Calculate ∇J according to (25);
  Update $[\theta(m), \omega(m)]$ according to (23) and set $m = m + 1$;
until $|J(\theta(m+1), \omega(m+1)) - J(\theta(m), \omega(m))| < \varepsilon$;
The resulting trajectory: $[\breve{\theta}, \breve{\omega}] = [\theta(m), \omega(m)]$;

Algorithm 2 Calculation of $\nabla S(t)$

Input: Time t, trajectories $[\theta(m), \omega(m)]$ and $S(t)$.

for $i = 1 : N$ **do**
  Get the length of vector $\theta_i(m)$, denoted by H;
  for $h = 1 : H$ **do**
    if $|\theta_{i(h+1)} - \theta_{ih}| > \frac{v_i^{\max 2}}{2C_i^a} + \frac{v_i^{\max 2}}{2C_i^d}$ **then**
      Calculate $\nabla t_{ih}^a, \nabla t_{ih}^u, \nabla t_{ih}^d, \nabla \theta_{ih}, \nabla \theta_{ih}^a, \nabla \theta_{ih}^d$ according to (44),(45),(46), (48),(49),(50), (51);
    else
      if $|\theta_{i(h+1)} - \theta_{ih}| \leq \frac{v_i^{\max 2}}{2C_i^a} + t_{ih}^d \frac{v_i^{\max 2}}{2C_i^d}$ **then**
        Calculate $\nabla t_{ih}^a, \nabla t_{ih}^u, \nabla t_{ih}^d, \nabla \theta_{ih}, \nabla \theta_{ih}^a, \nabla \theta_{ih}^d$ according to (54),(55),(56), (57),(58),(60), (61);
      end if
    end if
    Calculate $\nabla \omega_{ih}$ according to (41),(42);
    Calculate ∇t_{ih} according to (40);
  end for
end for
Calculate $\nabla S(t)$ according to (34),(36),(38),(39).

IV. Illustrative Examples

In this section, two simulation examples are presented for persistent monitoring in a 1-D space over 20s, using one and two agents respectively. Through these simulations, we are able to understand: 1) the optimal trajectory under second-order agent dynamics with physical constraints; 2) to verify the result of *Proposition 1*; and 3) to demonstrate the effectiveness of the gradient-based algorithm. The mission space $[0, 5]$ and the uncertainty dynamics of sampling points remain consistent in the two examples. The set of interested targets is $X = \{x_j\}, x_j = 0 + 0.25j, j = 1, 2, \ldots, M$, $M = 20$ with the increasing and decreasing rates $I(x_j) = 0.1$, $D(x_j) = 0.5$ respectively. The initial value of the uncertainty is $R(x_j, 0) = 0$. The effective sensing ranges of the two agents are $r_1 = r_2 = 1$. The maximum acceleration and deceleration are $C_i^a = 1, C_i^d = 1$. The maximum velocity $v_1^{max} = v_2^{max} = 1.5$. The error tolerance $\varepsilon = 1.0 \times 10^{-4}$ in the termination condition (24).

Algorithm 3 Collision avoid algorithm

In the simulation, there are three aspects that should be paid attention to: 1). The overflow problem. Since it is impossible to know the number of optimal dwelling points in advance, the dimensions of both $\theta_i(k)$ and $\omega_i(k)$ are unknown, it is, therefore, necessary to choose the dimensions large enough by using 0 to fill in at the end of the vectors; 2). The step-sizes $[\tilde{\theta}, \tilde{\omega}]$. Diminishing step-size should be applied as the performance metric is approaching to the optimal value; 3). The calculation of derivative. In the numerical simulations, in order to calculate $\dot{R}(s(t), x_j)$ in Algorithm 1, (6) is modified as follows. If $R(x_j, t_k) = 0$ and $I(x_j) - D(x_j)P(x_j, t_k) < 0$, $\dot{R}(x_j, t_{k+1}) = 0$. Otherwise, $\dot{R}(x_j, t_{k+1}) = I(x_j) - D(x_j)P(x_j, t_{k+1})$.

The simulation results of the two persistent monitoring examples are shown in Fig. 2 and Fig. 3 respectively.

In Fig. 2, the persistent monitoring task is executed by agent 1. Let $[\tilde{\theta}, \tilde{\omega}] = [0.04, 0.04]$ before 5th times iteration and $[\tilde{\theta}, \tilde{\omega}] = [0.02, 0.04]$ after 5th times iteration. The initial trajectory is $\theta(0) = [1.0, 4.0, 1.0, \ldots], \omega(0) = [0.3, 0.3, \ldots]$ shown by the dotted line in Fig. 2(a) and the optimal trajectory is denoted by the solid line in Fig. 2(a). The optimal velocity and acceleration of agent 1 are shown in Fig. 2(b) where $-1.5 \leq v_1(t) \leq 1.5$. From Fig. 2(b), in the acceleration or deceleration modes, $u_1(t) = \pm 1$ and in the maximal velocity or dwell modes $u_1(t) = 0$ which confirm the conclusion of *Proposition 1*. Moreover, compared with the simulation results in [22], the trajectory is smooth in this paper, and the velocity of agent is continuous. This demonstrates that our second order model better approximates reality. The performance metric decreases as iteration times increase in Fig. 2(c), which demonstrates the effectiveness of Algorithm 1. At the 12-th iteration, the performance metric $J_1(\theta(12), \omega(12)) = 4.053$ satisfies the terminal condition that $|J_1(\theta(12), \omega(12)) - J_1(\theta(11), \omega(11))| < \varepsilon$.

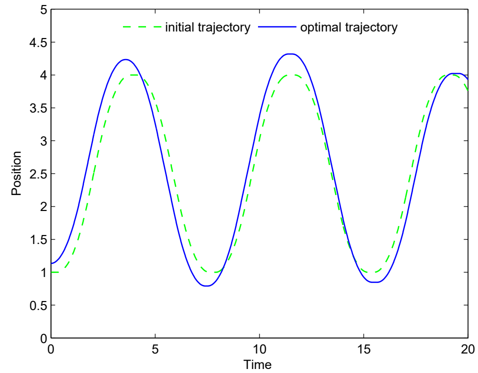

(a) Initial trajectory (green dash line) and optimal trajectory (blue) obtained by Algorithm 1

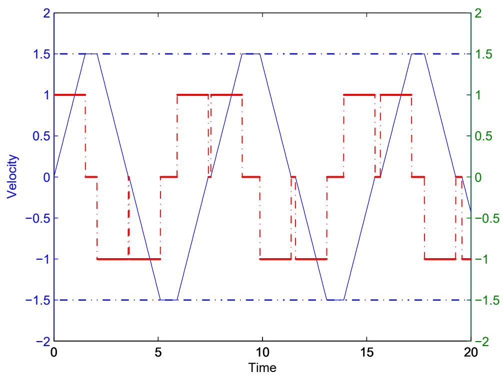

(b) Optimal velocity (blue) and acceleration (red) of agent 1

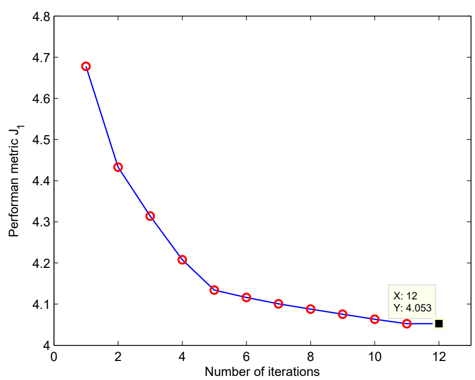

(c) Performance metric J_1 (decreases as the number of iterations increases)
Fig. 2. Persistent monitoring task executed by agent 1.

Fig. 3 shows the result of a persistent monitoring task executed by two agents. The iteration steps are $[\tilde{\theta}, \tilde{\omega}] = [0.02, 0.01]$ before the 20th iteration and $[\tilde{\theta}, \tilde{\omega}] = [0.008, 0.004]$ after the 20th iteration. The initial trajectories are $\theta_1(0) = [0.5, 2.0, 0.5, \ldots], \omega_1(0) = [0.2, 0.2, \ldots]$ and $\theta_2(0) = [3.0, 4.5, 3.0, \ldots], \omega_2(0) = [0.2, 0.2, \ldots]$ shown by the dotted line in Fig. 3(a) and the optimal trajectories are denoted by the solid line in Fig. 3(a). In this example, the optimal velocity and acceleration of agent 1 are shown in Fig. 3(b). Please note that the distances between the switching points do not satisfy conditions in Proposition 3, then the maximal velocity mode doesn't exist and the velocity of agent 1 cannot increase to v_1^{max}. The performance metric decrease as the increase of iteration times in Fig. 3(c), $J_2(\theta(23), \omega(23)) = 0.8865, |J_2(\theta(24), \omega(24)) - J_2(\theta(23), \omega(23))| < \varepsilon$. Comparing to Fig. 2(a), in Fig. 3(a) two agents have a better sensing capability than one agent. It is apparent that using two agents to complete the monitoring task leads to a smaller optimal performance metric in Fig. 3(c) that $J_2(\theta(12), \omega(12)) < J_1(\theta(24), \omega(24))$.

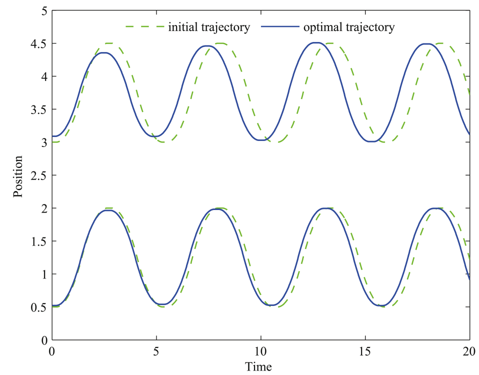

(a) Initial trajectory (green dash line) and optimal trajectory (blue) obtained by Algorithm 1

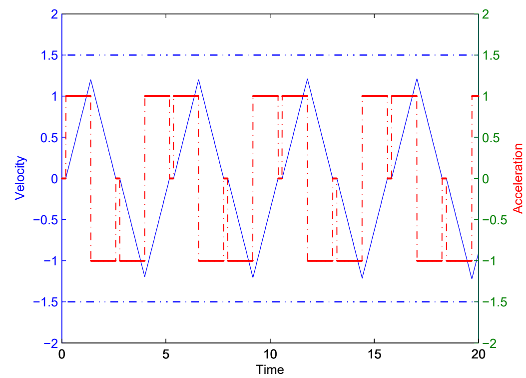

(b) Optimal velocity (blue) and acceleration (red) of agent 1

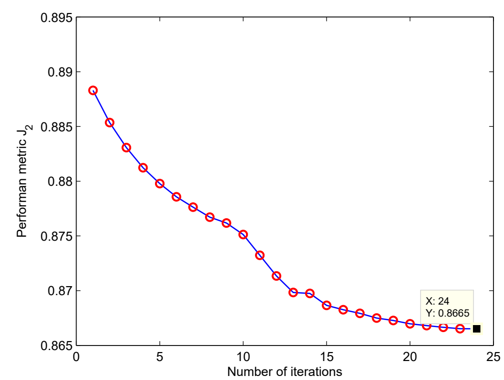

(c) Performance metric J_2 (decreases as the number of iterations increases)
Fig. 3. Persistent monitoring task executed by agent 1 and 2.

V. Conclusion

In this paper, optimal persistent monitoring tasks are performed via second-order multiple agents. The results of this paper bring persistent monitoring one step closer to realistic applications in the sense that the existing results are improved in two aspects, 1) the physical constraints on both the velocity and the acceleration are taken into consideration, 2) the control is on the acceleration leading to smooth agent trajectories. Our future work is to extend this model to 2D spaces or even with obstacles and possibly to control the agents in a distributed manner.

REFERENCES

[1] S. Alamdari, E. Fata, and S. L. Smith, "Persistent monitoring in discrete environments: Minimizing the maximum weighted latency between observations," *Int. J. of Robot. Research.*, vol. 33, no. 1, pp. 139–155, 2012.

[2] W. Meng, Z. He, R. Teo, and R. Su, "Integrated multi-agent system framework: decentralised search, tasking and tracking," *IET Contr. Theory and Appl.*, vol. 9, no. 4, pp. 493–502, 2014.

[3] D. Kingston, R. W. Beard, and R. S. Holt, "Decentralized perimeter surveillance using a team of uavs," *IEEE Trans. on Robot.*, vol. 24, no. 6, pp. 1394–1404, 2008.

[4] J. Yu, M. Schwager, and D. Rus, "Correlated orienteering problem and its application to informative path planning for persistent monitoring tasks," in *Proc. 26th IEEE/RSJ Int. Conf. Intell. Robots Syst.*, 2014, pp. 342–349.

[5] V. Srivastava and F. Bullo, "Stochastic surveillance strategies for spatial quickest detection," *Int. J. of Robot. Research*, vol. 32, no. 12, pp. 1438–1458, 2013.

[6] R. Reshma, T. Ramesh, and P. Sathishkumar, "Security situational aware intelligent road traffic monitoring using uavs," in *Proc. 2nd IEEE Int. Conf. VLSI Syst, Arch., Technol. Appl.*, 2016, pp. 1–6.

[7] H. Khurana, M. Hadley, N. Lu, and D. A. Frincke, "Smart-grid security issues," *IEEE Security & Privacy*, vol. 8, no. 1, 2010.

[8] V. C. Gungor, D. Sahin, T. Kocak, S. Ergut, C. Buccella, C. Cecati, and G. P. Hancke, "A survey on smart grid potential applications and communication requirements," *IEEE Transactions on Industrial Informatics*, vol. 9, no. 1, pp. 28–42, 2013.

[9] R. N. Smith, M. Schwager, S. L. Smith, B. H. Jones, D. Rus, and G. S. Sukhatme, "Persistent ocean monitoring with underwater gliders: Adapting sampling resolution," *J. Field Robot.*, vol. 28, no. 5, pp. 714–741, 2011.

[10] N. E. Leonard, D. A. Paley, R. E. Davis, D. M. Fratantoni, F. Lekien, and F. Zhang, "Coordinated control of an underwater glider fleet in an adaptive ocean sampling field experiment in monterey bay," *J. of Field Robot.*, vol. 27, no. 6, p. 718C740, 2010.

[11] D. E. Soltero, S. L. Smith, and D. Rus, "Collision avoidance for persistent monitoring in multi-robot systems with intersecting trajectories," in *Proc. 25th IEEE/RSJ Int. Conf. Intell. Robots Syst.*, vol. 32, no. 14, 2011, pp. 3645–3652.

[12] C. Song, L. Liu, G. Feng, and S. Xu, "Optimal control for multi-agent persistent monitoring," *Automatica*, vol. 50, no. 6, pp. 1663–1668, 2014.

[13] S. L. Smith, M. Schwager, and D. Rus, "Persistent monitoring of changing environments using a robot with limited range sensing," in *Proc. 28th IEEE Int. Conf. Robot. Autom.*, 2011, pp. 5448–5455.

[14] D. Portugal and R. P. Rocha, "Multi-robot patrolling algorithms: Examining performance and scalability," *Adv. Robot. J.*, vol. 27, no. 5, pp. 325–336, 2013.

[15] H. L. Choi and J. P. How, "Continuous trajectory planning of mobile sensors for informative forecasting ," *Automatica*, vol. 46, no. 8, pp. 1266–1275, 2010.

[16] J. Yu, M. Schwager, and D. Rus, "Correlated orienteering problem and it application to persistent monitoring tasks," *IEEE Trans. Robot.*, vol. 32, no. 5, pp. 1106–1118, 2016.

[17] N. Zhou, X. Yu, S. B. Andersson, and C. G. Cassandras, "Optimal event-driven multi-agent persistent monitoring of a finite set of targets," in *Proc. 55th IEEE Conf. Decision Contr.*, 2016, pp. 1814–1819.

[18] S. L. Smith, M. Schwager, and D. Rus, "Persistent robotic tasks: Monitoring and sweeping in changing environments," *IEEE Trans. Robot.*, vol. 28, no. 2, pp. 410–426, 2012.

[19] J. Yu, S. Karaman, and D. Rus, "Persistent monitoring of events with stochastic arrivals at multiple stations," *IEEE Trans. Robot.*, vol. 31, pp. 521–535, 2015.

[20] X. Yu, S. B. Andersson, N. Zhou, and C. G. Cassandras, "Optimal dwell times for persistent monitoring of a finite set of targets," in *2017 American Control Conference (ACC)*, 2017, pp. 5544–5549.

[21] X. Lin and C. G. Cassandras, "Trajectory optimization for multi-agent persistent monitoring in two-dimensional spaces," *IEEE Trans. Autom. Control*, pp. 1659–1664, 2015.

[22] C. G. Cassandras, X. Lin, and X. Ding, "An optimal control approach to the multi-agent persistent monitoring problem," *IEEE Trans. Autom. Control*, vol. 58, no. 4, pp. 947–961, 2013.

[23] H. Wei and S. Ferrari, "A geometric transversals approach to sensor motion planning for tracking maneuvering targets," *IEEE Trans. on Automatic Control*, vol. 60, no. 10, pp. 2773–2778, 2015.

[24] G. Foderaro, P. Zhu, H. Wei, T. A. Wettergren, and S. Ferrari, "Distributed optimal control of sensor networks for dynamic target tracking," *IEEE Trans. on Control of Net. Syst.*, vol. PP, no. 99, pp. 1–12, 2016.

[25] F. Pasqualetti, A. Franchi, and F. Bullo, "On cooperative patrolling: Optimal trajectories, complexity analysis, and approximation algorithms," *IEEE Trans. Robot.*, vol. 28, no. 3, pp. 592–606, 2012.

[26] M. Jadaliha and J. Choi, "Environmental monitoring using autonomous aquatic robots: Sampling algorithms and experiments," *IEEE Trans. Control Syst. Technol.*, vol. 21, no. 21, pp. 899–905, 2013.

[27] A. Jones, M. Schwager, and C. Belta, "Information-guided persistent monitoring under temporal logic constraints," in *Proc. 33rd Amer. Contr. Conf.*, 2015, pp. 1911–1916.

[28] G. Foderaro, S. Ferrari, and T. A. Wettergren, "Distributed optimal control for multi-agent trajectory optimization," *Automatica*, vol. 50, no. 1, pp. 149–154, 2014.

[29] S. Adlakha and M. Srivastava, "Critical density thresholds for coverage in wireless sensor networks," in *Proc. 3rd IEEE Wireless Commun. Networking Conf.*, vol. 3, 2003, pp. 1615–1620.

[30] R. F. Hartl, S. P. Sethi, and R. G. Vickson, "A survey of the maximum principles for optimal control problems with state constraints," *Siam Review*, vol. 37, no. 2, pp. 181–218, 2008.

[31] A. E. Bryson and Y. C. Ho, *Applied Optimal Control: Optimization, Estimation, and Control*. New York:Wiley, 1975.

[32] M. Athans and M. Canon, "On the fuel-optimal singular control of nonlinear second-order systems," *IEEE Trans. on Automatic Control*, vol. 9, no. 4, pp. 360–370, 1964.

[33] C. G. Cassandras, Y. Wardi, C. G. Panayiotou, and Y. Chen, "Perturbation analysis and optimization of stochastic hybrid systems," *Eur. J. Control*, vol. 16, no. 6, pp. 642–664, 2010.

Yan-Wu Wang (M10–SM13)received the B.S. degree in automatic control, the M.S. degree and the Ph.D. degree in control theory and control engineering from Huazhong University of Science and Technology (HUST), Wuhan, China, in 1997, 2000, and 2003, respectively. Currently, she is a Professor with the School of Automation, HUST, and with the Key Laboratory of Image Processing and Intelligent Control, Ministry of Education, China. Her research interests include hybrid systems, cooperative control, and multi-agent systems, with applications in smart grid.

Dr. Wang was a recipient of several awards, including the first prize of Hubei Province Natural Science in 2014, the first prize of the Ministry of Education of China in 2005, and the Excellent PhD Dissertation of Hubei Province in 2004, China. In 2008, she was awarded the title of "New Century Excellent Talents" by the Chinese Ministry of Education.

Yao-Wen Wei received the B.S. degree in 2015 from the school of Mathematics and Statistics, Huazhong University of Science and Technology (HUST), Wuhan, China. Currently, he is pursuing the M.S. degree from HUST. His research interests include optimization and persistent monitoring.

Xiao-Kang Liu received the B.S. degree in 2014 from the school of Automation, Huazhong University of Science and Technology (HUST), Wuhan, China. Currently, he is pursuing the Ph.D. degree from HUST. His research interests include output regulation, hybrid system, and smart grid.

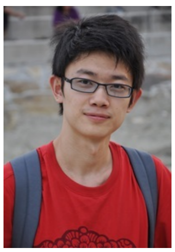

Nan Zhou received the B.S. degree in control science and engineering from Zhejiang University, Hangzhou, China, in 2011, the M.S. degree from Institute of Automation, Chinese Academy of Sciences, Beijing, China, in 2014. He is currently a Ph.D. candidate in systems engineering at Boston University, Boston, MA, USA. His research interests include optimal control of hybrid systems, cooperative control, and multi-agent systems, with applications in robotics, mobile sensor networks, and smart cities. He is a student member of the IEEE Control Systems Society and Robotics Automation Society.

Christos G. Cassandras (F'96) received the B.S. degree from Yale University, New Haven, CT, USA, in 1977, the M.S.E.E. degree from Stanford University, Stanford, CA, USA, in 1978, and the M.S. and Ph.D. degrees from Harvard University, Cambridge, MA, USA, in 1979 and 1982, respectively.

He was with ITP Boston, Inc., Cambridge, from 1982 to 1984, where he was involved in the design of automated manufacturing systems. From 1984 to 1996, he was a faculty member with the Department of Electrical and Computer Engineering, University of Massachusetts Amherst, Amherst, MA, USA. He is currently a Distinguished Professor of Engineering with Boston University, Brookline, MA, USA, the Head of the Division of Systems Engineering, and a Professor of Electrical and Computer Engineering. He specializes in the areas of discrete event and hybrid systems, cooperative control, stochastic optimization, and computer simulation, with applications to computer and sensor networks, manufacturing systems, and transportation systems. He has authored over 380 refereed papers in these areas, and five books.

Dr. Cassandras is a member of Phi Beta Kappa and Tau Beta Pi. He is also a Fellow of the International Federation of Automatic Control (IFAC). He was a recipient of several awards, including the 2011 IEEE Control Systems Technology Award, the 2006 Distinguished Member Award of the IEEE Control Systems Society, the 1999 Harold Chestnut Prize (IFAC Best Control Engineering Textbook), a 2011 prize and a 2014 prize for the IBM/IEEE Smarter Planet Challenge competition, the 2014 Engineering Distinguished Scholar Award at Boston University, several honorary professorships, a 1991 Lilly Fellowship, and a 2012 Kern Fellowship. He was the Editor-in-Chief of the IEEE TRANSACTIONS ON AUTOMATIC CONTROL from 1998 to 2009. He serves on several editorial boards and has been a Guest Editor for various journals. He was the President of the IEEE Control Systems Society in 2012.